2002 HST Calibration Workshop
Space Telescope Science Institute, 2002
S. Arribas, A. Koekemoer, and B. Whitmore, eds.

Optical Interferometry with *HST*/FGS at $V > 15$

E. Nelan and R. Makidon

Space Telescope Science Institute, 3700 San Martin Drive, Baltimore, MD, 21218

Abstract. The *Hubble Space Telescope*'s Fine Guidance Sensor FGS 1r has been used to observe cool white dwarf stars with apparent magnitudes that are near the FGS's faint limit. We had expected to discover that about 10% of these stars are binary white dwarf systems. We also expected the binaries to have angular separations much larger than the size of the FGS white light fringes, making them easy to resolve. Although we did find about 10% percent of the stars to be binaries, most have angular separations less than 25 mas, well below the *HST* diffraction limit. Instead of two widely separated fringes, we observed fringes that displayed subtle differences, in amplitude and morphology, from those of point sources. A major complication for our program was the need to address and remove the effects of the detector's dark current, which for the faintest targets contributed up to 40 percent of the counts. This paper outlines the process we employed to retrieve the science from the data.

1. Introduction

In Cycle 10 we used *HST* to observe cool white dwarf (WD) stars in an effort to discover binary systems composed solely of white dwarfs, hereafter referred to as double degenerate (DD) systems. We hoped to identify systems with separations suggesting orbital periods less than 25 years. Such binaries would be ideal candidates for follow up studies for deriving orbital elements, and ultimately the mass of each component. This would facilitate a more comprehensive calibration of the WD mass-radius relation and cooling curve for a variety of WD core and envelope compositions which are currently calibrated by only 4 WDs with dynamically measured masses. Based upon the incidence of binarity and the distribution of periods among G dwarf stars in the solar neighborhood (Duquennoy & Mayor 1991), and allowing for the expectation that systems with initial separations less than about 2 A.U. would evolve into unresolvable short period systems due to the orbital shrinkage expected to result from common envelope evolution (Iben & Livio 1993), we anticipated that about 10% of the WDs in our sample would be resolved as DDs with separations larger than 100 mas (all of the stars in our sample are within 50 pc). To optimize our prospects for resolving a DD, we restricted our target list to include only WDs cooler than about 9000 K since any companion could not be much cooler, and hence not much fainter than the primary.

Although we expected to discover DDs with separations wide enough to be resolved by WFPC2, the superior angular resolution achievable (8 mas) with the Fine Guidance Sensor 1r (FGS 1r) made it the instrument of choice in the event that binaries with small separations, or unfavorable projection angles might be encountered. However, the FGS 1r faint limit at $V = 17$ is set by the instrument's dark current. Many of the targets in our observing program would be fainter than $V = 16$, implying that the contribution from the dark counts would be comparable to that from the source. However, this presents an analysis problem only for binary systems with projected angular separations less than the size of the FGS white light fringe packet (50 mas). Few such systems were anticipated to be encountered.

2. Observations

We used FGS 1r in its high angular resolution observing mode (Transfer mode). After acquiring the star, the instrument's instantaneous field of view (IFOV) is scanned across the star's photocenter along a 45°diagonal path (in FGS X, Y detector space). The length of the scan is specified by the observer. We used scan lengths of 1 asec and step sizes of 0.8 mas. The total number of scans (typically 50) was set by the length of the observing window (we specified the maximum number possible). Each step in the scan is a 25 msec integration. The data contains the 40 Hz measurement of the location of the FGS 1r IFOV and the photon counts from the instrument's four photomultiplier tubes (PMTs). These data are used to reconstruct the target's observed fringes along the FGS 1r X, Y axis. For a detailed description and discussion of the FGS, please consult the *FGS Instrument Handbook* and the *HST Data Handbook for the FGS*, both of which can be obtained from the FGS web site (follow the links from http://www.stsci.edu/hst/fgs.)

3. Analysis

Data from the individual scans are auto correlated, binned, and co-added to produce a pair of high signal to noise ratio (SNR) interferograms for the observation, one for each of the instrument's two orthogonal baselines. The photon noise in the individual scans for stars fainter than $V = 15.5$ makes the auto correlation unreliable as it injects false jitter. In such cases the scans are correlated using the *HST* guide star data (from the guiding FGSs) prior to being binned and co-added. After co-adding, the interferograms are smoothed by application of a cubic spline.

If an object is resolved by FGS 1r to be a binary system, the observed fringes will depart from those obtained from a point source. To analyze binary star observations, one finds the best fitting linear superposition of point source fringes which have been scaled and shifted to represent the relative brightness and separation of the two sources comprising the binary system. The data along the FGS X-axis are analyzed independently from those along the Y-axis, however the relative brightness of the components must agree.

The point source fringes are available from observations of standard stars made as part of the *HST*/FGS calibration program. For the best SNR, only bright standards are observed ($V < 10$, generally). However, when observing a star as faint as $V = 16.4$, the instrument dark current contributes about 40 percent of the counts accumulated by the detector. Since this is incoherent with the light from the star, the fringe visibility is reduced, as can be seen in Figure 1 which compares the observed fringes of two point sources, one at $V = 11.5$ and the other at $V = 16.4$. Clearly, before any headway can be made in analyzing the data from scans of faint stars, the effect of the dark counts must be addressed. Rather than trying to remove the dark counts from the faint star data, it is better to use the data from a bright calibration source to model the fringes of a faint point source. In other words, we scale the observed photometric counts of the bright standard down to the level they would be had the star been as faint as the science target, we add in the dark counts, and then regenerate the fringes. Figure 2 shows the bright star fringe after being adjusted to simulate a $V = 16.4$ point source, and compares it to the observed fringes of the faint source.

4. Results

In this section we show how our analysis of the observed fringes of the faint, $V = 16.2$ star WD1818+126 has allowed us to resolve it as a binary system. Bergeron et al. (1997) note that the object's spectra is best modeled as a composite from two stars, a DA and a cooler DC, to explain the shallow depth of the hydrogen lines. They also note that the inferred

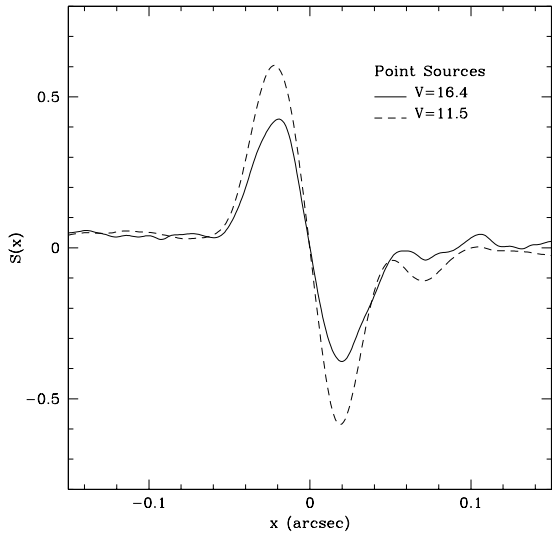

Figure 1. Comparison of fringes from two point sources, one at $V = 11.5$, the other at $V = 16.4$. The dark counts have reduced the amplitude of the faint star's fringes.

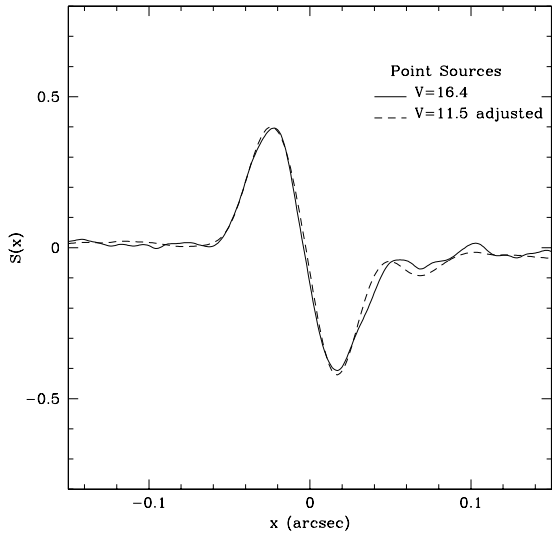

Figure 2. The bright star fringe, after being adjusted as if it can from a faint source, is compared to the observed fringes of a faint source.

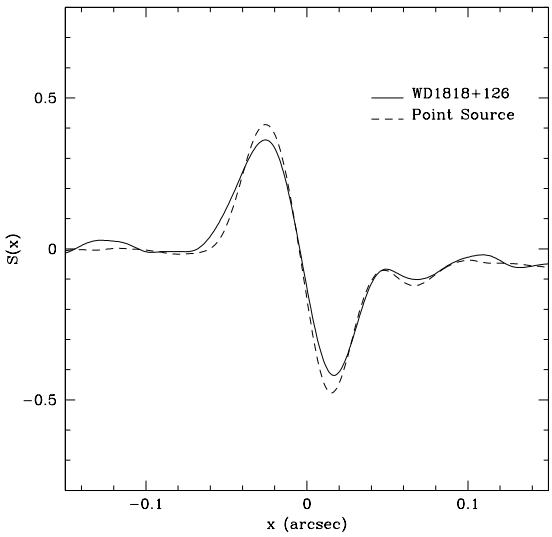

Figure 3. Comparison of an adjusted $V = 11.5$ fringe to that of WD1818+126. This shows that the white dwarf is not a point source.

surface gravity (derived from its luminosity and temperature) is too low, implying either an unusually low mass (large radius) or that it is a binary system composed of white dwarfs.

Figure 3 compares the observed fringes of WD1818+126 to those from a bright point source which has been modeled as a faint star. Clearly WD1818+126 is not a point source. Figure 4 compares the fit of a model which uses the adjusted calibration fringe to determine the separation and relative brightness of the components along the FGS X-axis. Figure 5 shows the model's fit along the FGS 1r Y-axis. The object is a wide binary with separation of 176 mas, but its position angle was nearly aligned with the FGS 1r Y-axis, thereby projecting a small separation along the X-axis and a large, easily resolved separation along the Y-axis. The best fitting model yields an angular separation along (X, Y)=(15.7, 173.7) mas, with the secondary being 0.94 magnitudes fainter than the primary. Note that the faint companion is nearly $V = 17$, very close to the FGS 1r's limiting sensitivity.

5. Conclusions

We had expected to detect only wide DDs, such as WD1818+126. However, the wide systems turned out to be fewer in number than the close (sep<30 mas) systems. The chance alignment of WD1818+126 as projected onto the FGS 1r yields a wide, easily resolved separation along the Y-axis and a small, sub-diffraction-limited separation along the X-axis. The Y-axis result clearly established the binary nature of the object. This in turn firmly establishes the reliability of the analysis process which resulted in the X-axis detection. Therefore, we conclude that performance of FGS 1r is not significantly impaired near the instrument's faint limiting magnitude, and that sub-diffraction-limited angular resolution remains viable, provided the dark counts are properly modeled.

The prevalence of binary white dwarf systems with projected angular separations suggesting physical separations less than 1 A.U. indicates that common envelope evolution does not necessarily result in unresolvable short period binary systems with small physical separations. This has implications for the range of values that can be taken on by the common envelope efficiency parameter α_{CE}. Finally, our program to identify DD systems suitable for follow up studies for dynamical mass determinations has yielded several good candidates.

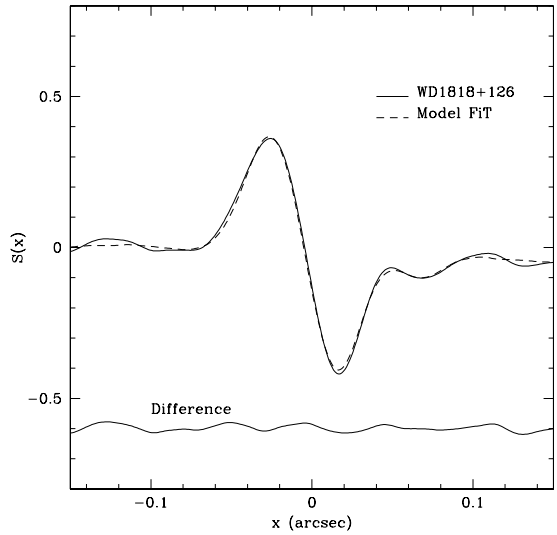

Figure 4. The FGS 1r X-axis fringe of WD1818+126 is best modeled as a composite of two point sources with a projected angular separation of 15.7 mas and a magnitude difference of 0.94.

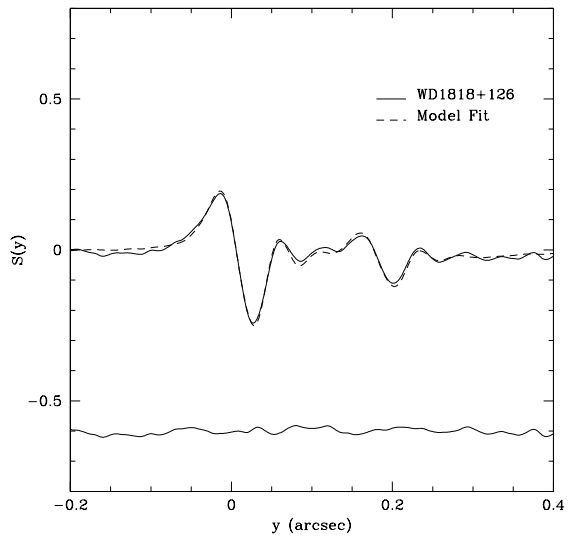

Figure 5. The wide projected angular separation of WD1818+126's components along the FGS 1r Y-axis leave no doubt that this is a binary system. The measured magnitude difference agrees well with the result from the analysis of the X-axis data.

It is important for *HST* to continue observing the longer period systems ($P > 15$ years) in order to establish an accurate baseline for a hand off to SIM in the event that SIM's mission lifetime is otherwise too short for deriving the orbital elements of these systems.

Acknowledgments. This work is based upon observations made with the NASA/ESA *Hubble Space Telescope*, which is operated by the Space Telescope Science Institute, of the Association of Universities for Research in Astronomy, Inc. under NASA contract NAS5-26555. This work is supported through grant GO-09169 (E. Nelan, P.I.)

References

Bergeron, P., Ruiz, M. T., & Leggett, S. K. 1997, ApJS, 108

Duquennoy, A. & Mayor, M. 1991, A&A, 248,485

Iben, I. & Livio, M. 1993, PASP, 105, 13731